STRUCTURE AND SOOT FORMATION PROPERTIES OF LAMINAR FLAMES

A. M. El-Leathy, F. Xu and G. M. Faeth
Department of Aerospace Engineering
The University of Michigan
Ann Arbor, Michigan

INTRODUCTION

Soot formation within hydrocarbon-fueled flames is an important unresolved problem of combustion science for several reasons: soot emissions are responsible for more deaths than any other combustion-generated pollutant, thermal loads due to continuum radiation from soot limit the durability of combustors, thermal radiation from soot is mainly responsible for the growth and spread of unwanted fires, carbon monoxide emissions associated with soot emissions are responsible for most fire deaths, and limited understanding of soot processes in flames is a major impediment to the development of computational combustion. Motivated by these observations, soot processes within laminar premixed and nonpremixed (diffusion) flames are being studied during this investigation. The study is limited to laminar flames due to their experimental and computational tractability, noting the relevance of these results to practical flames through laminar flamelet concepts. Nonbuoyant flames are emphasized because buoyancy affects soot processes in laminar diffusion flames whereas effects of buoyancy are small for most practical flames (refs. 1-7).

This study involves both ground- and space-based experiments, however, the following discussion will be limited to ground-based experiments because no space-based experiments were carried out during the report period. The objective of this work was to complete measurements in both premixed (refs. 8-10) and nonpremixed (refs. 11-13) flames in order to gain a better understanding of the structure of the soot-containing region and processes of soot nucleation and surface growth in these environments, with the latter information to be used to develop reliable ways of predicting soot properties in practical flames. The present discussion is brief, more details about the portions of the investigation considered here can be found in refs. 8-13.

EXPERIMENTAL METHODS

Measurements in premixed flames were completed along the axis of a 60 mm diameter water-cooled porous-plug flat flame burner directed vertically upward, involving a total of twelve different fuel-rich ethylene/air and methane/oxygen flames at atmospheric pressure. Measurements in nonpremixed flames were completed along the axis of flames produced by a coflowing jet burner directed vertically upward with a 35 mm fuel port and a 60 mm inner diameter air port operating at atmospheric pressure. A total of six nonpremixed flames were studied, involving acetylene, ethylene, propylene and propane as fuels.

Measurements in both premixed and nonpremixed flames were as follows: soot volume functions using deconvoluted laser extinction, flow temperatures using deconvoluted multiline emission, soot structure using thermophoretic sampling and TEM analysis, concentrations of major gas species using sampling and gas chromatography, concentrations of some radical species (H, OH and O) using the deconvoluted Li/LiOH atomic absorption technique and streamwise velocities using laser velocimetry.

RESULTS AND DISCUSSION

Soot and Flame Structure. All soot particles were the same as observed in earlier work in diffusion flames (refs. 1-7). They consisted of roughly spherical primary particles that were monodisperse at each flame condition and collected into mass fractal aggregates having large variations of the number of primary particles per aggregate.

Samples of premixed flame structure can be found in refs. 8-10, present considerations will be limited to properties along the axis of a typical diffusion flame as illustrated in Fig. 1 for an ethylene-fueled flame. Flow velocities increase with distance due to effects of buoyancy, yielding a nonlinear variation of residence time with distance. Effects of radiant heat loss are substantial yielding a relatively flat temperature distribution with maximum values well below adiabatic flame temperatures. Primary soot particle diameters reach a maximum early in the soot formation region due to combined effects of soot nucleation, growth and oxidation. The original fuel eventually disappears due to effects of decomposition, oxidation and soot formation (the last being relatively minor). Robust fuel-like species, however, persist throughout the soot formation region, e.g., C_2H_2, C_2H_4, CH_4 and H_2. Concentrations of radicals, e.g., H, OH and O, increase as the flame sheet is approached. The soot formation region does not approach equilibrium concentrations similar to premixed flames (refs. 8-10), however, but exhibits superequilibrium ratios generally in excess of 10.

Soot Surface Growth. Measured soot surface growth rates were corrected for effects of soot oxidation, similar to past studies of soot growth in this laboratory (refs. 2-4,6,7). Reported values of corrected soot growth, however, were limited to conditions where estimated soot oxidation rates never exceeded half the gross soot surface growth rate. Soot surface growth rates, w_g, were interpreted using the Hydrogen-Abstraction-Carbon-Addition (HACA) soot growth mechanisms of Frenklach and coworkers (refs. 14-16) and Colket and Hall (ref. 17).

To a first approximation $w_g \sim [H][C_2H_2]$, where [i] denotes the concentration of the species i, for the HACA soot growth mechanisms of refs. 14-17. This behavior is illustrated in Fig. 2 in order to provide a direct test of the main features of the HACA soot growth mechanisms, without the intrusion of uncertainties due to the numerous empirical parameters of the detailed HACA mechanisms of refs. 14-17, based on measurements in premixed and diffusion flames (refs. 8-12). The correlation for the various flame conditions is quite good, and improves when actual HACA mechanisms are used, which is encouraging.

The corresponding evaluation of the HACA mechanism of soot surface growth due to Colket and Hall (ref. 17) is illustrated in Fig. 3, where R_{CH} denotes the value of reaction rate expression of this approach (and unknown steric factor in the model has a very reasonable value of 0.9). The overall correlation illustrated in Fig. 3 is seen to be reasonably effective for both premixed and diffusion flames. Results using the HACA mechanism of Frenklach and coworkers (refs. 14-17) were similar, see ref. 17.

Soot Nucleation. Soot nucleation is complex but a reasonable hypothesis is that it is dominated by the rate of formation of large molecular weight soot precursor species whose rates of formation should be somewhat similar to rates of soot surface growth, leading to a potential soot nucleation rate correlation $w_n = k_n(T)[C_2H_2][H]$, where the rate constant k_n was sought as an Arrhenius expression in terms of the temperature T. Available measurements of soot primary particle nucleation rates measured in premixed and diffusion flames (refs. 8-12) are illustrated in Fig. 4. This yields a scattered correlation with results for premixed and diffusion flames behaving in similar manner. Improved methods that achieve less scattered results are needed, however, that properly account for the detailed chemical and physical processes responsible for soot nucleation.

ACKNOWLEDGMENTS

This research was sponsored by NASA Grants NAG3-2048 and –2404, under the technical management of D. L. Urban of the Glenn Research Center, Cleveland, Ohio.

REFERENCES

1. Sunderland, P.B., Mortazavi, S., et al., *Combust. Flame* 96:97 (1994).
2. Sunderland, P.B., Köylü, Ü.Ö. and Faeth, G.M., *Combust. Flame* 100:310 (1995),
3. Sunderland, P.B. and Faeth, G.M., *Combust. Flame* 105:132 (1996),
4. Lin, K.-C., Sunderland, P.B. and Faeth, G.M., *Combust. Flame* 104:369 (1996).
5. Urban, D.L. et al., *AIAA J.* 36:1346 (1998).
6. Lin, K.-C. et al., *Combust. Flame* 116:415 (1999),
7. Lin, K.-C. and Faeth, G.M., *AIAA J.* 37:759 (1999).
8. Xu, F., Sunderland, P.B. and Faeth, G.M., *Combust. Flame* 108:1471 (1997),
9. Xu, F., Lin, K.-C. and Faeth, G.M., *Combust. Flame* 115:195 (1998),
10. Xu, F. and Faeth, G.M., *Combust. Flame* 121:640 (2000),
11. Xu, F. and Faeth, G.M., *Combust. Flame*, in press.
12. El-Leathy, A.M., Xu, F. and Faeth, G.M., *Combust. Flame*, in preparation.
13. Xu, F., El-Leathy, A.M. and Faeth, G.M., *Combust. Flame*, submitted.
14. Frenklach, M. and Wang, H., *Proc. Combust. Inst.* 23:1589 (1990).
15. Frenklach, M. and Wang, H., *Soot Formation in Combustion* (H. Bockhorn, ed.), Springer-Verlag, Berlin, 1994, p. 165.
16. Kazakov, A.,Wang, H. and Frenklach, M., *Combust. Flame* 100:111 (1995).
17. Colket, M.B. and Hall, R.J., *Soot Formation in Combustion* (H. Bockhorn, ed.), Springer-Verlag, Berlin, 1994, p. 442.

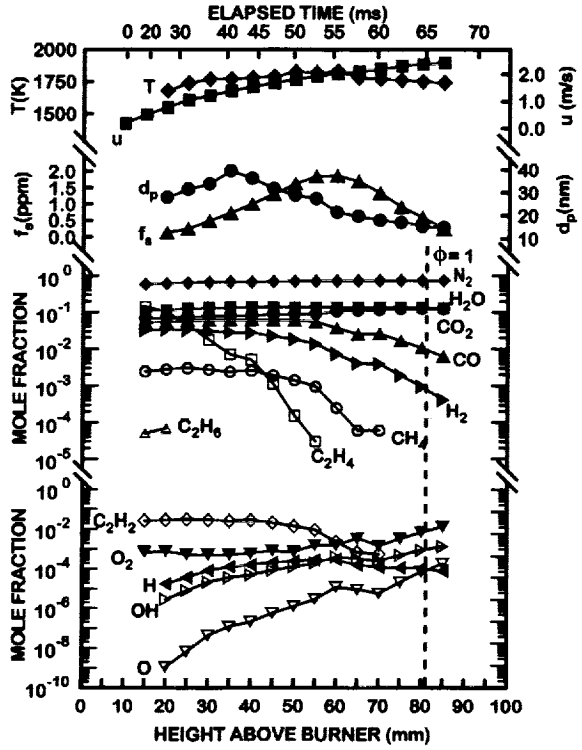

Fig. 1. Measured soot and flame properties along the axis of an ethylene/air laminar jet diffusion flame at atmospheric pressure.

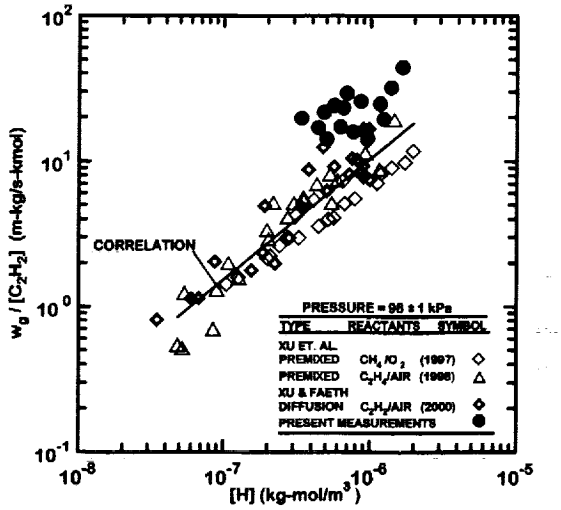

Fig. 2. Soot surface growth rates (corrected for soot oxidation) as a function of acetylene and hydrogen-atom concentrations for laminar premixed and diffusion flames at atmospheric pressure. Measurements from refs. 8-12.

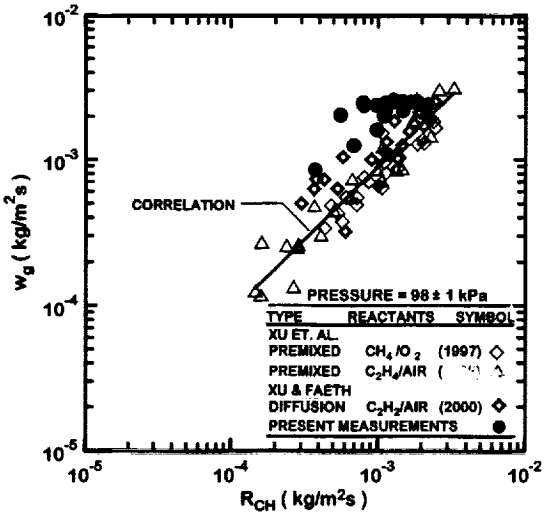

Fig. 3. Soot surface growth rates (corrected for soot oxidation) in terms of the HACA mechanism of Colket and Hall (ref. 17) for laminar premixed and diffusion flames at atmospheric pressure. Measurements from refs. 8-12.

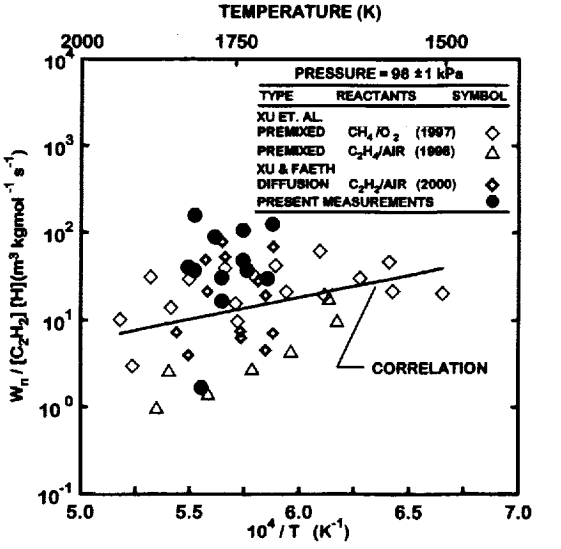

Fig. 4. Soot nucleation rates as a function of acetylene concentrations, hydrogen-atom concentrations and temperatures for laminar premixed and diffusion flames at atmospheric pressure. Measurements from refs. 8-12.